http://dx.doi.org/10.1016/j.jmb.2012.08.021 J. Mol. Biol. (2012) 423, 687–701

Contents lists available at www.sciencedirect.com

Journal of Molecular Biology

journal homepage: http://ees.elsevier.com.jmb

Kinetics and Thermodynamics of Phenotype: Unwinding and Rewinding the Nucleosome

Andrew H. Mack[1,2]†, Daniel J. Schlingman[1,3]†, Robielyn P. Ilagan[3], Lynne Regan[1,3,4]* and Simon G. J. Mochrie[1,2,5]*

[1]*Integrated Graduate Program in Physical and Engineering Biology, Yale University, New Haven, CT 06520, USA*
[2]*Department of Applied Physics, Yale University, New Haven, CT 06520, USA*
[3]*Department of Molecular Biophysics and Biochemistry, Yale University, New Haven, CT 06520, USA*
[4]*Department of Chemistry, Yale University, New Haven, CT 06520, USA*
[5]*Department of Physics, Yale University, New Haven, CT 06520, USA*

Received 27 June 2012;
received in revised form
23 August 2012;
accepted 24 August 2012
Available online
31 August 2012

Edited by K. Morikawa

Keywords:
chromatin;
single molecule;
optical tweezers;
free energy;
nucleosome

Chromatin "remodeling" is widely accepted as the mechanism that permits access to DNA by the transcription machinery. To date, however, there has been no experimental measurement of the changes in the kinetics and thermodynamics of the DNA–histone octamer association that are required to remodel chromatin so that transcription may occur. Here, we present the results of optical tweezer measurements that compare the kinetic and thermodynamic properties of nucleosomes composed of unmodified histones with those of nucleosomes that contain a mutant histone H4 (H4-R45H), which has been shown to allow SWI/SNF remodeling factor-independent transcription from the yeast *HO* promoter *in vivo*. Our measurements, carried out in a force-clamp mode, determine the force-dependent unwinding and rewinding rates of the nucleosome inner turn. At each force studied, nucleosomes containing H4-R45H unwind more rapidly and rewind more slowly than nucleosomes containing unmodified H4, indicating that the latter are the more stable. Extrapolation to forces at which the winding and unwinding rates are equal determines the absolute free energy of the nucleosome inner turn to be $-32k_BT$ for nucleosomes containing unmodified H4 and $-27k_BT$ for nucleosomes containing H4-R45H. Thus, the "loosening" or "remodeling" caused by this point mutation, which is demonstrated to be sufficient to allow transcriptional machinery access to the *HO* promoter (in the absence of other remodeling factors), is $5k_BT$. The correlation between the free energy of the nucleosome inner turn and the sin (*S*WI/SNF-*in*dependent) transcription suggests that, beyond partial unwinding, complete histone unwinding may play a role in transcriptional activation.

Introduction

Histones and other proteins assemble eukaryotic DNA into a hierarchy of structures collectively called chromatin. The fundamental organizational unit of chromatin is the nucleosome, in which 146 base pairs of DNA are wound around a protein complex composed of two copies each of the core histones H2A, H2B, H3, and H4. For gene activation, nucleosomes must be displaced to permit transcrip-

**Corresponding authors.* Integrated Graduate Program in Physical and Engineering Biology, Yale University, New Haven, CT 06520, USA. E-mail addresses: lynne.regan@yale.edu; simon.mochrie@yale.edu.

† A.H.M. and D.J.S. contributed equally to this work.

Abbreviations used: PTM, posttranslational modification; EDTA, ethylenediaminetetraacetic acid; TPM, tethered particle motion; QPD, quadrant photodiode.

tion factors to bind to the DNA. Thus, chromatin is not only a remarkable packaging strategy but also a dynamic structure that changes to regulate access to specific genes at specific times.[1]

Histone variants and modifications, independently or in concert with ATP-dependent chromatin remodeling enzymes, such as SWI/SNF, are believed to promote the remodeling of chromatin that is required for transcription.[2] In yeast, an upstream regulatory sequence (*URS1*) of the *HO* promoter contains a strong nucleosome positioning sequence, which requires remodeling by SWI/SNF for transcription to occur.[3–5] Sternberg *et al.* used a genetic screen to identify mutations that allow transcription from the *HO* locus, even in the absence of SWI/SNF.[6] A number of sin (*S*WI/SNF-*in*dependent) mutations map to the globular domains of histones H3 and H4 and restore transcription from the *HO* locus to wild-type levels.[7–11] The simplest interpretation of these results is that the mutant histones destabilize the nucleosome, allowing access to the DNA in the absence of additional remodeling factors (Fig. 1a–c). Measuring the kinetic and thermodynamic differences between a wild-type nucleosome and a nucleosome containing sin mutant histones quantifies the reduction in nucleosome stability that is sufficient to allow transcription *in vivo* without the requirement for SWI/SNF.

Several groups have pioneered the use of optical or magnetic tweezers to study the properties of nucleosomes.[12–22] Brower-Tolland *et al.* proposed a model for nucleosome unwinding/rewinding under force in which there are four distinct states (Fig. 1d).[14] In state 2, nearly two turns of DNA are wrapped around the histone octamer in the canonical nucleosome structure.[23] In state 1, the outer turn of DNA is unwound, but the inner turn remains intact. In state 0, both the outer and the inner turns are unwrapped, but the histone octamer remains bound to the DNA. Finally, the histone octamer is dissociated from the DNA. References 15, 18, and 19 confirm Brower-Tolland *et. al.*'s model and establish unambiguously that nucleosomes under tension unwind in a stepwise fashion, in contrast to force-independent measurements,[24,25] with the nucleosome outer turn unwinding at forces beyond about

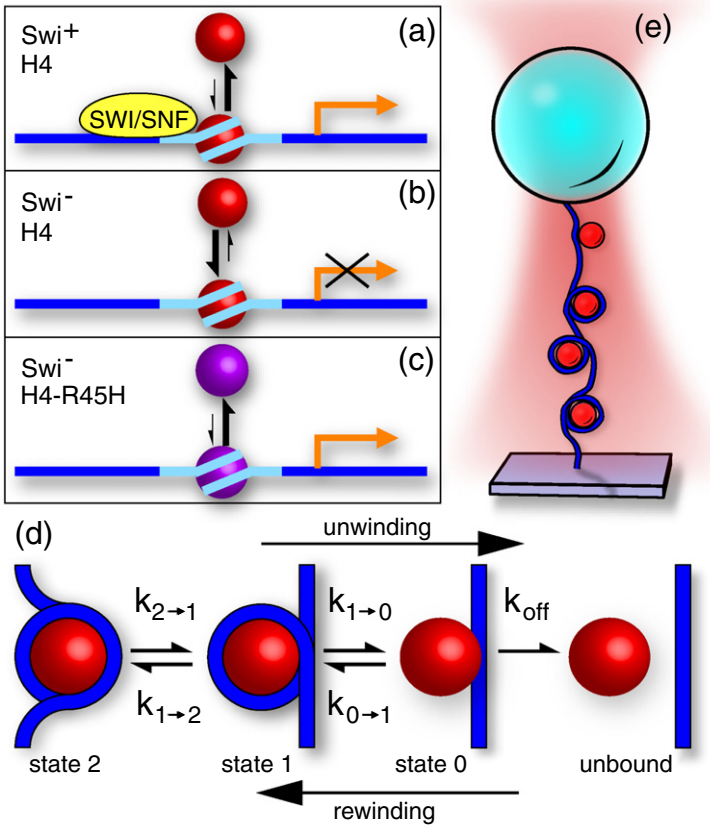

Fig. 1. (a–c) Schematic illustration of the *URS* of the yeast *HO* promoter, model for nucleosome unwinding/rewinding, and a schematic of the optical tweezers setup. (a) Wild-type yeast with a functional SWI/SNF complex (yellow) and nucleosomes containing H4 (red spheres). DNA is shown in blue with *URS1* in pale blue. Nucleosomes are displaced from the *URS1* by the SWI/SNF complex. Nucleosome occupancy is decreased (black arrows) allowing transcription (orange arrow). (b) Mutant yeast lacking a functional SWI/SNF complex, with nucleosomes containing H4. Nucleosome occupancy is increased, inhibiting transcription. (c) Mutant yeast lacking a functional SWI/SNF complex, with nucleosomes containing sin mutant H4-R45H. Nucleosome occupancy is decreased, and transcription is restored to levels comparable to wild-type yeast. (d) The four microstates for nucleosome unwinding/rewinding proposed in Ref. 14. Histones are red. DNA is blue. For state 2, the nucleosome is fully wrapped by nearly two turns of DNA. For state 1, the outer turn is unwrapped, but the inner turn is wrapped. For state 0, both the outer and the inner turns are unwrapped, but the histone octamer remains bound to the DNA. Finally, the histones may be unbound from the DNA. (e) Schematic of the experimental design. DNA (thick blue line) containing 601 positioning sequences[42] tethers a polystyrene bead (turquoise sphere) to a glass slide (mauve rectangle). Arrays of nucleosomes (red spheres) are created *in situ*. Force is applied in the axial direction using optical tweezers (red beam).

2 pN and with the nucleosome inner turn unwinding beyond about 7 pN. Moreover, the existence of discrete states has been explained theoretically by Kulic and Schiessel, who showed that the elasticity of a nucleosomal DNA superhelix under tension gives rise to a force-dependent free-energy barrier between the described states, inhibiting gradual unwinding.[26] Recent experiments on single nucleosomes reconstituted with core histones from chicken erythrocytes reveal that the nucleosome hops between states 1 and 2 at forces near 3 pN, yielding an absolute binding free energy of the nucleosome outer turn of $-12k_BT$ (-7.3 kcal/mol).[18,19] However, the absolute binding free energy of the nucleosome inner turn has not previously been measured.[27] Here, therefore, we focus on the nucleosome inner turn, and using single-molecule optical tweezer measurements, we compare the kinetics and thermodynamics of unwinding and rewinding of the nucleosome inner turn for nucleosomes containing wild-type H4 (henceforth H4) with nucleosomes containing a sin mutant H4, in which arginine 45 is mutated to histidine (henceforth H4-R45H). Additional novel aspects of this study include measurement of the absolute force-dependent unwinding ($k_{1\to0}$) and rewinding ($k_{0\to1}$) rates of the nucleosome inner turn, neither of which has been measured previously. A number of ATP-dependent chromatin "remodeling" enzymes, such as SWI/SNF,[28] exert force on DNA to displace bound nucleosomes. Therefore, the behavior of nucleosomes under tension and their mechanical properties, more generally, are highly relevant to our understanding of the regulation of nucleosomes *in vivo*. Combining these measurements permits us to determine the absolute binding free energy of the nucleosome inner turn. We observe significant differences in the kinetic rate constants and absolute free energies between the different nucleosome types. Nucleosomes containing H4-R45H unwind more rapidly and rewind more slowly at all forces tested, establishing a physical difference between nucleosomes containing wild-type H4 that require the action of SWI/SNF to be removed from the *HO URS1* and nucleosomes containing H4-R45H that abrogate this requirement. Thus, our study is the first to quantify the extent to which histone–DNA interactions must be "loosened" to allow transcription.[29]

Results

Nucleosomes containing sin mutant histones unwind faster than nucleosomes containing wild-type histones

Our experimental approach is to measure the extension of nucleosome-bound DNA as a function of time while holding the force constant—a force clamp. We compare the unwinding/rewinding behavior of nucleosomes (Fig. 1e) containing H4 and nucleosomes containing H4-R45H over a wide range of forces. Such measurements allow us to observe individual nucleosome unwinding/rewinding events and to compare directly the behavior of each type of nucleosome at the same force. In Fig. 2a, we show extension *versus* time measurements at a constant force for nucleosomes containing H4 (red) and nucleosomes containing H4-R45H (blue). Both profiles display eight stepwise jumps in extension of approximately 25 nm. Each jump corresponds to unwinding the inner turn of DNA from one nucleosome, that is, the transition from nucleosome state 1 to nucleosome state 0 of Fig. 1d. In these traces, nucleosomes containing H4-R45H unwind more rapidly than those containing H4.

To combine and analyze multiple traces measured at the same force, we determine the time of every unwinding event in all traces (see Materials and Methods for further details). At each force, this collection of unwinding times determines the fraction of nucleosome inner turns unwound as a function of time. The stepwise continuous lines in

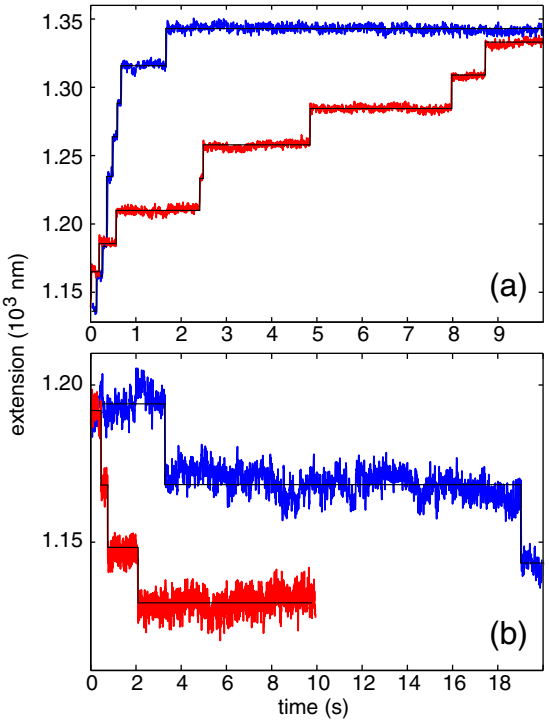

Fig. 2. Comparison of the extension *versus* time measured at fixed force for nucleosomes containing either H4 (red) or H4-R45H (blue). (a) Unwinding at 11.3 pN. Stepwise increases in extension correspond to the transition from state 1 to state 0. (b) Rewinding at 3.8 pN. Stepwise decreases correspond to the transition from state 0 to state 1. The black lines in (a) and (b) correspond to the steps identified by our step-finding procedure.

Fig. 3a show the fraction unwound *versus* time for nucleosomes containing H4 at three different forces. Each step in these composite curves corresponds to an individual unwinding event. Similarly, the stepwise continuous lines in Fig. 3b show the fraction unwound *versus* time for nucleosomes containing H4-R45H at the same three forces. These data span 3 orders of magnitude in time and include unwinding events that occur within 0.1 s and beyond 300 s of reaching the force clamp. At each force shown, it is evident that nucleosomes containing H4-R45H unwind faster than those containing H4. To determine the unwinding rate $k_{1\to0}$, at the force in question, we assume first-order kinetics. Therefore, the probability that a nucleosome initially in state 1 has unwound to state 0 at time t after initiation of the force clamp is given by

$$p = 1-e^{-k_{1\to0}t} \quad (1)$$

To compare Eq. (1) to our measurements, we calculate the value of $k_{1\to0}$ that maximizes the probability of the measured distribution of unwinding times, as described in detail in Materials and Methods. The broken lines in Fig. 3a and b correspond to Eq. (1) calculated using these maximum-likelihood values of $k_{1\to0}$. In each case, the measured fraction unwound *versus* time is consistent with first-order kinetics, suggesting that all nucleosomes occupy identical, independent binding sites.

Nucleosomes containing sin mutant histones rewind more slowly than nucleosomes containing wild-type histones

We also characterized nucleosome rewinding by monitoring nucleosomes initially in the unwrapped state (state 0) transitioning to the singly wrapped state (state 1) at a fixed force. Figure 2b shows extension *versus* time measurements at a constant force for nucleosomes containing H4 (red) or H4-R45H (blue). It is clear here that nucleosomes containing H4-R45H rewind more slowly than nucleosomes containing H4. The protocol followed to collect these data involves clamping the force to 15 pN for 1 s, which is sufficiently long to be confident that no nucleosomes remain wound. Then, we rapidly decrease the force to the force of interest and hold it fixed at that value. By monitoring the accompanying stepwise decreases in extension, we measure nucleosome rewinding at this fixed force. An unavoidable complication with this procedure is that, in state 0, nucleosomes may

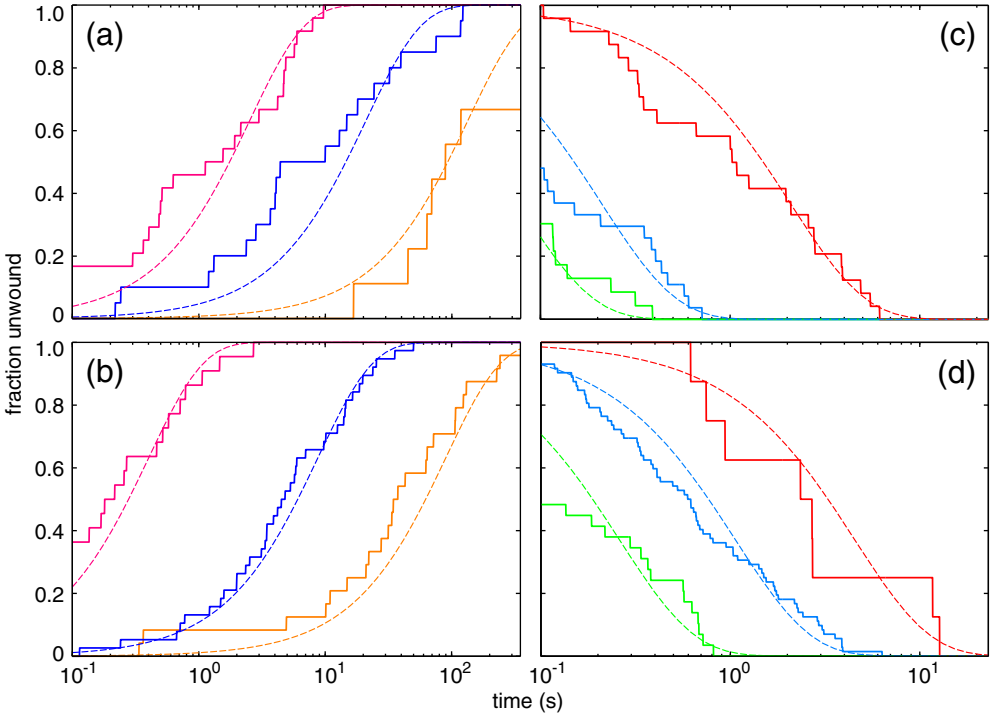

Fig. 3. Cumulative fraction of nucleosomes unwound *versus* time at several forces. (a) Unwinding for nucleosomes containing H4 at 6.6 pN (orange continuous line), 8.5 pN (blue continuous line), and 11.3 pN (magenta continuous line). (b) Unwinding for nucleosomes containing H4-R45H at same forces as (a). (c) Rewinding for nucleosomes containing H4 at 1.9 pN (green continuous line), 2.8 pN (cyan continuous line), and 3.8 pN (red continuous line). (d) Rewinding for nucleosomes containing H4-R45H at same forces as (c). Broken lines in (a) and (b) correspond to Eq. (1) using the maximum-likelihood values of the unwinding rates. Broken lines in (c) and (d) correspond to Eq. (2) using the maximum-likelihood values of the rewinding rates.

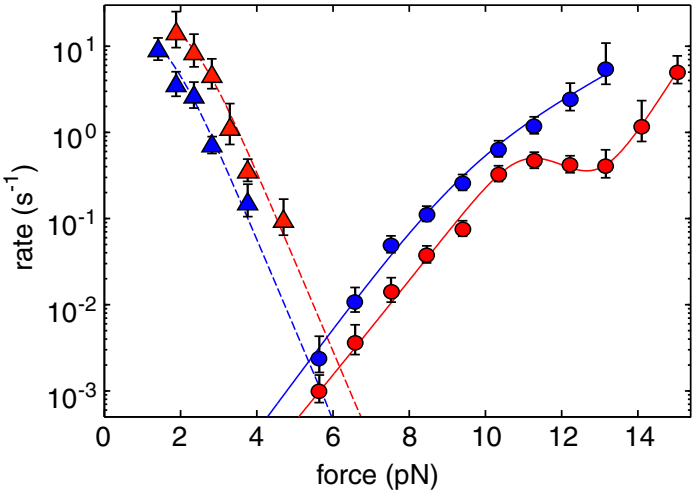

Fig. 4. Comparison of unwinding and rewinding rates as a function of force for nucleosomes containing H4 (red) and H4-R45H (blue). The unwinding rates are shown as circles and rewinding rates are shown as triangles. The continuous (unwinding) and broken (rewinding) lines are included as guides to the eye. Errors shown are 1 SD, equal to the rate divided by the square root of the number of measured events.

dissociate, leading to a diminished number of DNA-bound nucleosomes, but nevertheless, we are able to measure rewinding on multiple constructs at each force studied and determine the rewinding times using an algorithm similar to that used for unwinding. This procedure yields a collection of rewinding times, which determines the fraction of nucleosome inner turns remaining unwound as a function of time. The stepwise continuous lines in Fig. 3c show the fraction unwound as a function of time for nucleosomes containing H4 at three different forces. Data measured at the same forces, but for nucleosomes containing H4-R45H, are shown in Fig. 3d. At each force tested, nucleosomes containing H4-R45H rewind more slowly than those containing H4.

To determine the rewinding rate $k_{0\to1}$, we again assume first-order kinetics. Therefore, the probability that a nucleosome initially in state 0 remains in state 0 at time t after initiation of the force clamp is given by

$$p = e^{-k_{0\to1}t} \qquad (2)$$

Similarly to unwinding, we determine the maximum-likelihood value of $k_{0\to1}$. The broken lines in Fig. 3c and d show Eq. (2), using the corresponding maximum-likelihood values of $k_{0\to1}$. The measured fractions unwound again show good agreement with first-order kinetics [Eq. (2)] with deviations within the range expected from counting statistics, as discussed in more detail in Materials and Methods.

The absolute binding free energy of the inner turn of nucleosomes containing H4-R45H is less than that of nucleosomes containing H4

Figure 4 summarizes our measurements of the rates of unwinding and rewinding. For all forces studied, nucleosomes containing H4-R45H unwind more rapidly and rewind more slowly than those containing H4. For both types of nucleosome, the rewinding rates decrease rapidly as the force increases. Conversely, for nucleosomes containing H4-R45H, the unwinding rate increases with force over the entire range of forces measured. For nucleosomes containing H4, the unwinding rate increases with force up until about 10 pN. In the region between about 10 and 13 pN, the unwinding rate is virtually independent of force before increasing again after 13 pN. Unwinding rates that increase rapidly with increasing force we ascribe to free-energy barriers that are the result of localized histone–DNA interactions.[21] By contrast, a weak force-dependent unwinding rate is a signature of the DNA elastic free-energy barrier to unwinding proposed in Refs. 26 and 30.

Free energy of the nucleosome inner turn

At each force tested, nucleosomes containing H4-R45H unwind more rapidly and rewind more slowly than nucleosomes containing H4, indicating that nucleosomes composed of wild-type histones are the more stable. In fact, using the data shown in Fig. 4, we are able to determine the free energy of the nucleosome inner turn as follows.

As described in detail in Ref. 31, there are three contributions to the force-dependent Gibbs free-energy difference between state 0 and state 1 (ΔG_{total}). The first contribution is the free energy of the nucleosome inner turn ($\Delta G_{0\to1}$). The second is the work done by the nucleosome on the optical trap, W. The third ($\Delta G_{\text{stretch}}$) is a small contribution associated with stretching the DNA tether. Thus, we have

$$\Delta G_{\text{total}} = \Delta G_{0\to1} + W + \Delta G_{\text{stretch}} \qquad (3)$$

It is shown in Ref. 32 that, for force (F) and temperature (T),

$$W + \Delta G_{\text{stretch}} = -F(L_1 - L_0)\left(1 - \sqrt{\frac{k_B T}{F L_P}}\right) \qquad (4)$$

where L_P is the DNA's persistence length, L_1 is the contour length of the non-nucleosomal DNA when the nucleosome is in state 1, and L_0 is the contour length of the non-nucleosomal DNA when the nucleosome is in state 0. In writing Eq. (4), we have taken the DNA's persistence length to be the same for all nucleosome states.[19] Furthermore, for DNA with contour length L, the DNA's extension x is related to the force via[32]

$$x = L\left(1-\sqrt{\frac{k_BT}{4FL_P}}\right) \tag{5}$$

It follows that

$$W + \Delta G_{stretch} = -F(x_1-x_0)\frac{1-\sqrt{\frac{k_BT}{FL_P}}}{1-\sqrt{\frac{k_BT}{4FL_P}}} = Fd\frac{1-\sqrt{\frac{k_BT}{FL_P}}}{1-\sqrt{\frac{k_BT}{4FL_P}}} \tag{6}$$

where $d=x_0-x_1$, and x_0 and x_1 are the DNA's extensions in state 0 and state 1, respectively.

The Gibbs free-energy difference between state 1 and state 0 is also related to the rates of unwinding and rewinding by

$$\Delta G_{total} = -k_BT\ln\frac{k_{0\to1}}{k_{1\to0}} \tag{7}$$

Therefore, at the force at which the unwinding rate and the rewinding rate are equal, we have

$$\Delta G_{total} = 0 \tag{8}$$

Calling this force F^*, it follows from Eqs. (3), (6), and (8) that the free energy of the nucleosome inner turn is given by

$$\Delta G_{0\to1} = -F^*d\frac{1-\sqrt{\frac{k_BT}{F^*L_P}}}{1-\sqrt{\frac{k_BT}{4F^*L_P}}} \tag{9}$$

Extrapolating the rates in Fig. 4 to the forces at which the unwinding and rewinding rates are equal, we determine F^* to be 6.0±0.3 pN for nucleosomes containing H4 and 5.1±0.3 pN for nucleosomes containing H4-R45H. It follows that the absolute free energies of the nucleosome inner turn are −32.4±1.8k_BT (−19.2±1.0 kcal/mol) for nucleosomes containing H4 and −27.0±1.7k_BT (−16.1±1.0 kcal/mol) for nucleosomes containing H4-R45H. (We use d=23.5±0.5 nm for nucleosomes containing H4 and d=23.2±0.5 nm for nucleosomes containing H4-R45H.) Thus, decreasing the free energy of the DNA inner turn–histone octamer interaction by 5k_BT is sufficient to allow transcription.

Discussion

We have presented a comprehensive study of the unwinding and rewinding rates of the nucleosome inner turn for strictly defined, homogeneous nucleosomes. We have found that nucleosomes containing H4-R45H unwind faster and rewind more slowly than those containing H4. From these rates, we have determined that the absolute free energy of the nucleosome inner turn is greater than that of the nucleosome outer turn by a factor of about two and one-half, suggesting that unwinding the inner turn is the major barrier to nucleosome remodeling. [We note, however, that a precise comparison is not possible because of the different buffer conditions used in Ref. 18 (10 mM Tris–acetate, 50 mM potassium acetate, 10 mM magnesium acetate, 1 mM DTT, and 0.1 mg/ml bovine serum albumin) and in this work (10 mM Hepes, pH 7.4; 100 mM NaCl; 1 mg/ml casein; and 0.1% Tween).]

We have also found that the absolute free energy of the inner turn for nucleosomes containing H4-R45H is 5.4±1.5k_BT (3.2±0.9 kcal/mol) greater than that of those containing H4, implying that a nucleosome containing H4-R45H is about 200-fold more likely to be unwound than a nucleosome containing H4. The sin mutant H4-R45H was identified in yeast because it allowed transcription from the *HO* locus without the requirement for SWI/SNF. Thus, our measurements reveal a direct, and we assume causal, relationship between a biological phenotype and the kinetic and thermodynamic properties of nucleosomes. Specifically, we have quantified, for the first time, what it means for a modification or variant to "loosen" the histone–DNA interaction sufficiently to allow transcription to proceed. The direct correlation between the binding free energy of the nucleosome inner turn and the change in transcription in the absence of SWI/SNF in yeast has important implications for transcriptional mechanisms, suggesting that, beyond partial unwinding, complete histone unwinding may play a role in transcriptional activation.

A key hypothesis that has emerged in the last decade is the histone code hypothesis,[33,34] which posits that histone posttranslational modifications (PTMs)[35,36] such as acetylation, phosphorylation, methylation, or ubiquitination (alone or in combinations) constitute a set of instructions for which genes to express. Two broad molecular mechanisms, which are probably not mutually exclusive, for the role of histone PTMs have been hypothesized.[37] So-called *cis* mechanisms correspond to PTMs that directly change the interactions between histones and DNA. For example, acetylation of lysines or arginines in histones' unstructured tails decreases the positive charge of the tail. As a result, it is proposed that the histones have decreased affinity for negatively charged DNA, facilitating transcription. Alternatively, *trans* mechanisms propose that histone PTMs are

specifically recognized by nonhistone factors, which either themselves modify chromatin structure or recruit additional factors that do so.

For example, methylation is recognized by chromo-like domains of the Royal family (chromo, tudor, MBT) and by PHD domains, acetylation is recognized by bromodomains, and phosphorylation is recognized by a domain within 14-3-3 proteins.[37] To truly understand these processes, it is essential to deconvolute the different contributions of both *cis* and *trans* effects. In addition to site-specific PTMs of the canonical histones, each core histone, except for histone H4, exhibits a number of nonallelic isoforms, called histone variants, with sequences and/or expression patterns that can differ strikingly from their canonical counterparts. These histone variants constitute another important route to chromatin-based regulation of genomic properties.[38–40] Despite the clear importance of histone PTMs and histone variants, the physical effects of these changes and how they ultimately relate to gene expression have not yet been elucidated.[41] The measurements presented in this paper for nucleosomes containing unmodified histones and for nucleosomes containing unmodified H2A, H2B, H3, and sin mutant H4-R45H open the way for future quantitative measurements of the effects of histone PTMs and histone variants on nucleosome unwinding and rewinding kinetics and thermodynamics. Therefore, they serve as key benchmarks against which the kinetics and free energies of nucleosomes containing histones with PTMs or variants may be compared.

Materials and Methods

DNA preparation

As a gift from Dr. Daniela Rhodes, we received plasmids containing 12 tandem repeats of the 601 nucleosome positioning sequence.[42,43] We use this DNA to assemble regularly spaced nucleosomes, separated by short regions of linker DNA. We prepare large quantities (1 mg) of these plasmids using standard procedures. For "carrier" DNA, we use commercial ultrapure salmon sperm DNA, sheared to about 1000-base-pair fragments (Invitrogen). To assemble nucleosomes arrays for optical tweezer measurements, we employed the 601 nucleosome positioning sequence,[42,43] both to be certain that the nucleosomes bind at identical sites with a defined binding affinity and to facilitate comparisons with the results of other researchers. However, of the 72 central bases in the 601 sequence, 36 are identical with the corresponding bases in the *HO URS1* nucleosome positioning sequence.[5,44]

Recombinant histone expression and purification

Our goal to measure the free-energy difference between nucleosomes of specified composition requires the use of recombinant histones to be certain of the exact composition of every single molecule that we study. pET-11 plasmids containing genes for *Xenopus laevis* histones H2A, H2B, H3, or H4, under control of a T7 promoter, were received as a gift from Dr. Karolin Luger. Site-directed mutagenesis (QuikChange™ site-directed mutagenesis kit, Stratagene) was used to introduce the R45H mutation into H4.[45–47] The mutation was confirmed by DNA sequencing. Purification followed published protocols.[48] In brief, the cell pellet from a 1-l culture was resuspended in 30 ml of wash buffer [50 mM Tris (pH7.4), 100 mM NaCl, 1 mM ethylenediaminetetraacetic acid (EDTA), and 1% Triton X-100]. The cells were then lysed by sonication, and the soluble and insoluble fractions were separated by centrifugation. The insoluble pellet was washed by resuspension in wash buffer, sonication, and centrifugation two times more. The pellet was washed twice more with wash buffer without Triton X-100. The final pellet was soaked in 120 μl dimethyl sulfoxide and incubated for 30 min at room temperature. A 5-ml volume of unfolding buffer [20 mM Tris (pH7.6), 7 M guanidinium hydrochloride (GuHCl), and 10 mM DTT] was added, and the mixture was incubated for 1 h at room temperature with shaking. Insoluble materials were removed by centrifugation, and the supernatant was collected and dialyzed using Slide-A-Lyzer Dialysis Cassette with 3500 Da cutoff (Thermo Scientific) overnight at room temperature into urea dialysis buffer [10 mM Tris (pH8), 8 M urea, 100 mM NaCl, 1 mM EDTA, and 5 mM β-mercaptoethanol] to exchange from GuHCl to urea, prior to ion-exchange chromatography. After dialysis, any precipitant was removed by centrifugation and discarded. Following dialysis, the solution was passed over an 8-ml Q-Sepharose fast flow column (Amersham Biosciences) and the flow-through, containing histones, was collected. The flow-through was then loaded onto a 5-ml Hi-Trap SP-Sepharose fast flow column (Amersham Biosciences), pre-equilibrated with urea buffer [10 mM Tris (pH8), 7 M urea, 200 mM NaCl, 1 mM EDTA, and 5 mM β-mercaptoethanol] at a flow rate of 2 ml/min. The sample in the column was washed with three-column volumes of urea buffer. Histone protein was then eluted using urea buffer plus 600 mM NaCl. Fractions were collected and purity was assessed by sodium dodecyl sulfate polyacrylimide gel electrophoresis (SDS-PAGE). Fractions containing suitably pure histone were combined, dialyzed into double-distilled water, and then lyophilized and stored as dry powder at −80 °C.

We use these methods to express and purify unmodified H2A, H2B, H3, and H4 and mutant H4-R45H. We routinely assemble and purify histone octamers from these materials. Figure 5 shows the reconstitution of histone octamers from purified recombinant H2A, H2B, H3, and H4 and from purified recombinant H2A, H2B, H3, and H4-R45H.

Surface attachment strategy

Unique functional groups must be incorporated at each end of a piece of double-stranded DNA in order to tether the DNA between a bead and a surface. The interaction between digoxigenin-modified DNA and anti-digoxigenin antibodies is commonly used as one attachment group, and the interaction between biotin-modified DNA and

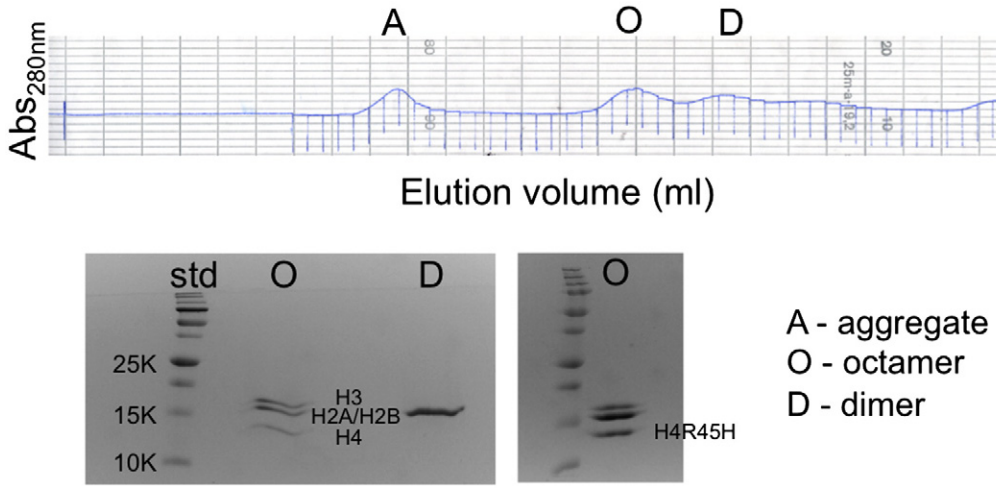

Fig. 5. Histone octamers reconstituted from recombinant *X. laevis* H2A, H2B, H3, and H4 or H4-R45H. Top: Gel-filtration chromatograph showing the separation of pure histone octamers (O) from aggregate (A) and H2A–H2B dimers (D). In this reconstitution, more H2A and H2B were used than H3 and H4; thus, excess H2A–H2B dimer is visible (D). Bottom left: SDS-PAGE analysis of the gel-filtration fraction containing histone octamers (O) and the gel-filtration fraction containing H2A–H2B dimers (D) from the reconstitution using H2A, H2B, H3, and H4. The same reconstitution method was used to prepare histone octamers containing H4-R45H. Bottom right: SDS-PAGE analysis of the gel-filtration fraction containing histone octamers (O) from the reconstitution using H2A, H2B, H3, and H4-R45H.

streptavidin is used as the other. Under our solution conditions, the biotin–streptavidin interaction is sufficiently strong to remain bound during the duration of our experiments for the necessary range of forces.[49] The interaction between digoxigenin-modified DNA and anti-digoxigenin antibodies, however, is not mechanically robust, as carefully shown in Ref. 50. When we used an anti-digoxigenin–digoxigenin linkage to tether the DNA to the surface, we found that the tether lifetime was shorter than required to perform the desired experiments.

To solve this problem, we invented an alternative attachment strategy, described in detail in Ref. 51. In brief, we incorporate a modified nucleotide that contains a reactive amine group, at one end of the DNA. We coat a glass coverslip with silane-polyethylene glycol *N*-hydroxysuccinamide under nonaqueous conditions then react the modified surface with the modified DNA. The single reactive amine group on the DNA reacts with the *N*-hydroxysuccinamide to form a covalent bond. This method yields robust DNA tether attachment. Using this attachment method, it is possible to carry out DNA force-clamp measurements at forces exceeding 15 pN for many minutes without detachment.

Tethered particle motion (TPM)[52] was used as a diagnostic to identify and select singly tethered beads for subsequent optical trapping measurements. Specifically, DNA-tethered beads were viewed via video microscopy, and their thermal Brownian motion were recorded and tracked for 400 s using the particle tracking software‡. Beads that explore a noncircular region, indicating the existence of multiple tethers, were immediately eliminated from consideration.

‡available at http://www.physics.georgetown.edu/matlab/

Reconstitution of histone octamers

Histone octamers were prepared following published protocols.[48] Briefly, each lyophilized histone protein was dissolved at a concentration of approximately 2 mg/ml in unfolding buffer [20 mM Tris (pH7.5), 6 M GuHCl, and 5 mM DTT] and incubated for at least 30 min at room temperature. The concentration of each core histone was measured using UV absorbance at 278 nm. The denatured histones were then mixed in an equimolar ratio, and the total protein concentration was adjusted to 1 mg/ml using unfolding buffer. The mixture was dialyzed into refolding buffer [10 mM Tris (pH7.5), 2 M NaCl, 1 mM EDTA, and 5 mM β-mercaptoethanol]. After dialysis, any insoluble material was removed by centrifugation. The solution was then loaded onto a Superdex S200 16/60 gel-filtration column (Amersham Biosciences), pre-equilibrated with refolding buffer. Fractions were analyzed by SDS-PAGE and those fractions containing pure octamer were pooled and concentrated to 17 μM using an Amicon™ Centricon™ with 3500 Da cutoff. Pure octamer was stored at 4 °C. This procedure serves to ensure the assembly of histone octamer and to separate the pure octamer from dimers and aggregates, as shown in Fig. 5.

Reconstitution of nucleosomes on sheared salmon sperm carrier DNA

Purified histone octamer was mixed with sheared salmon sperm carrier DNA (Invitrogen) in a 1:1 ratio of octamer to 200 base pairs of DNA in a high-salt buffer [10 mM Tris–HCl (pH7.5), 2 M NaCl, 1 mM EDTA, and 5 mM β-mercaptoethanol]. This solution was slowly dialyzed, using a continuous buffer exchange setup, into a low-salt buffer [10 mM Tris–HCl (pH7.5), 10 mM NaCl, and 1 mM EDTA] over a period of 24 h at 4 °C.[48] The

assembled nucleosomes were further dialyzed into 10 mM Tris–HCl buffer (pH7.5) and 1 mM EDTA. The so-obtained nucleosomes were stored at 4 °C and used within 1 month. To verify nucleosome assembly, we performed a DNA mobility shift assay on a small aliquot of the sample.[53] A glycerol-only loading buffer was used and the gel was stained with ethidium bromide after electrophoresis.

In situ nucleosome assembly

In many previous optical tweezer studies of chromatin, nucleosomal arrays were created *ex situ* and then flowed into the chamber, where optical or magnetic tweezers experiments were performed. By contrast, we reconstitute nucleosomes *in situ*, following an assembly strategy that is a variation of the route followed in Ref. 53.

Nucleosomes on carrier DNA were diluted to a concentration of 250 nM octamer in 10 mM Hepes (pH7.4), 680 mM NaCl, 1 mg/ml casein, and 0.1% (v/v) Tween. The nucleosomes were then flowed into the flow cell and incubated for 30 min to allow for transfer of nucleosomes from the carrier salmon sperm DNA to the tethered 601 array DNA. Nucleosome transfer was monitored using TPM.[52] The buffer in the flow cell was then exchanged with 10 mM Hepes (pH7.4), 100 mM NaCl, 1 mg/ml casein, and 0.1% (v/v) Tween. Optical tweezer experiments were conducted under these solution conditions.

Multiple checks confirm that we are properly assembling nucleosome arrays *in situ*:

1. Ensemble biochemical methods (gel electrophoresis mobility shifts) show that nucleosome arrays containing either H4 or H4-R45H form reliably using our procedures (data not shown).
2. Optical tweezer measurements of the force *versus* extension curves of our *in situ* reconstituted nucleosome arrays (Figs. 6 and 7) reproduce the signature features of nucleosome arrays.[14–19]
3. Force-clamp traces (Fig. 2) and force *versus* extension traces (Figs. 6 and 7) reveal steps in length of 21–26 nm, consistent with those reported in Refs. 14, 15, 18, and 19 for unwinding the nucleosome inner turn.
4. The measured fraction of nucleosome inner turns unwound or rewound at each force is consistent with a single-exponential function of time, suggesting that all nucleosomes are bound to equivalent sites.

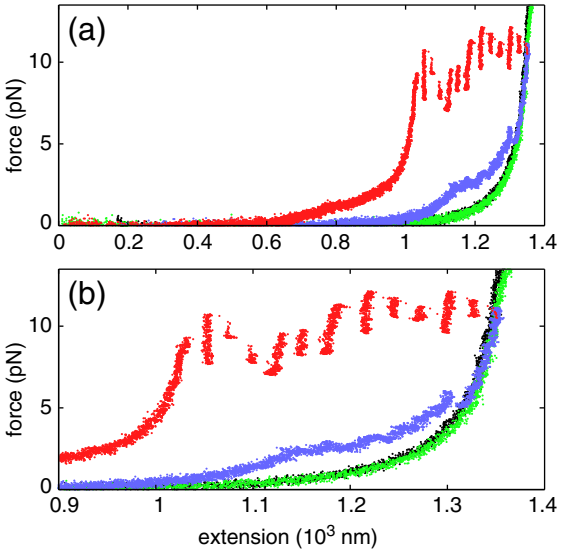

Fig. 6. Comparison of force *versus* extension profiles for a nucleosome array (red and blue), reconstituted as described in the text, with force *versus* extension profiles of naked DNA (green and black). (a) The profiles over the entire range of extensions studied. (b) Detailed behavior for extensions greater than 900 nm. The red and green traces correspond to extending the DNA. The blue and black traces correspond to relaxing the DNA.

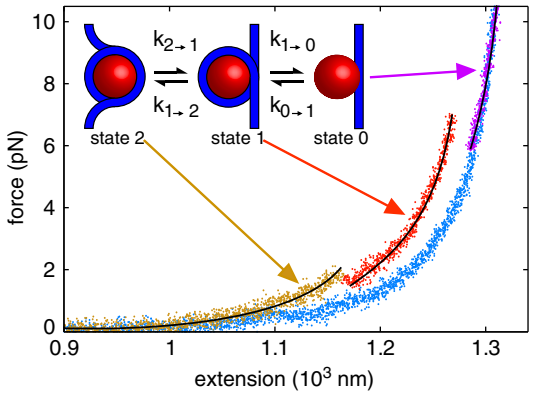

Fig. 7. Force *versus* extension trace of a mononucleosome. The mononucleosome starts in state 0 and is then relaxed (blue trace). Subsequently, the nucleosome is stretched (tan, red, and purple trace). Initially, in state 2 (tan segment of the trace), the nucleosome is wrapped by almost two turns of DNA. With increasing force, the nucleosome transitions from state 2 to state 1. In state 1 (red segment of the trace), the outer turn is unwrapped, but the inner turn remains wrapped. With further increase in the force, the nucleosome transitions from state 1 to state 0. In state 0 (purple segment of the trace), the DNA is unwrapped, but the histone octamer remains bound to the DNA. These features reproduce the canonical mononucleosome force *versus* extension traces of Refs. 18 and 19.

Optical trapping experiments

In the optical tweezer setup used for these experiments, the 2.5-mm-diameter beam from a high-stability, 3-W, 1064-nm laser (Laser Quantum, Stockport, UK) was incident on an acousto-optic deflector (IntraAction DTD-274HA6) to optically isolate the laser from the downstream optics train, ensuring stability, and to control the trapping laser power. Located between the acousto-optic deflector and the microscope objective (Nikon CFI 100×,

oil immersion, NA 1.25) is a telescope arrangement that expands the beam diameter by a factor of three, ensuring that the back pupil of the microscope objective is overfilled, as required for strong trapping. Beyond the objective, the beams are directed onto a quadrant photodiode (QPD) (Phresh Photonics SiQu50-M), located in a plane conjugate to the back focal plane of the microscope condenser lens. In such a conjugate plane, the total intensity in all four QPD quadrants is linearly proportional to the displacement of a trapped bead from the center of the trap along the beam direction. At the same time, the difference in intensity between the two left and the two right quadrants and between the top and the bottom quadrants is proportional to the displacement of the bead from the center of its trap in the corresponding directions transverse to the beam. This method of determining bead position—"back-focal-plane interferometry"[54]—provides a sensitive measure of the force on the bead because force is proportional to the bead displacement. Calibrations were performed using the power spectrum method.[55] To visualize the tethered beads, we used a CMOS camera (Thorlabs) with Kohler illumination provided by a diode emitting superbright blue light (Phillips Lumileds LUXEON™).

Our setup incorporates a laminar flow cell that permits the fluid around the tether to be exchanged via computer-controlled syringe pumps (OEM syringe pump; Harvard Apparatus). Our flow cell is mounted on a piezoelectric stage (NanoMAX311; Thorlabs) permitting us to vary the tether position relative to the laser focus and, thus, to vary the tension in the tether.

We employed an optical tweezer assay, in which force is applied to surface-tethered DNA in a direction perpendicular to the surface of the microscope coverslip (Fig. 1e). Advantages of this axial geometry include that it is relatively straightforward to implement a robust and reliable feedback loop, which maintains the force at a fixed value, namely, a force clamp. In addition, it is straightforward to measure the absolute length of the chromatin or DNA. Alternative implementations that also apply force in the axial direction are described in Refs. 56 and 57; beads tethered via a single DNA molecule were selected using TPM, as described above, and centered in an optical trap using the piezoelectric stage by minimizing the QPD difference signal in both transverse directions.

Force-extension measurements

We carried out force *versus* extension measurements to verify that our nucleosome arrays reproduce the behavior observed previously.[12–20] Figure 6 shows a force *versus* extension trace obtained while increasing the extension at a constant velocity. A nucleosome array was extended to nearly full extension for the first time (red trace) and then relaxed (blue trace). Also shown in Fig. 6 are naked DNA traces, shown in green for increasing extension and black for decreasing extension. Figure 6a shows the traces over the entire range of extensions studied, from zero extension, at which point the bead touches the surface of the microscope coverslip, to the maximum extension of about 1350 nm. Figure 6b highlights the jumps in length that occur for nucleosome-array extensions between 900 and 1350 nm. The nucleosome-array traces are different for extension (red) and relaxation (blue). On stretching the nucleosome array for the first time (red trace), for extensions between about 800 and 1000 nm, there is an approximate plateau in which the force increases weakly with increasing extension. In this region, a 22-nm length of DNA is inferred to unwind from each nucleosome in a statistically smooth fashion, as each nucleosome transitions from state 2 to state 1.[14] This transition appears to be smooth in the force *versus* extension trace of Fig. 6 because the outer turn unwinding/rewinding rates are such that nucleosomes are hopping back and forth between states 2 and 1, sampling both states 2 and 1 through the relevant portion of the trace. Beyond about 1000 nm, the force increases rapidly with increasing extension and the force *versus* extension curve shows a number of successive jumps, each involving an increase in the DNA length of 25 nm, corresponding to the transition of a nucleosome from state 1 to state 0. In the red trace, there are 12 jumps before the full extension of the DNA is reached, indicating that 12 nucleosomes were initially bound to the DNA in this case. These data reproduce the force *versus* extension curves of nucleosome arrays obtained previously—see Fig. 1d of Ref. 14 for example. Subsequent relaxation yields the force *versus* extension trace, shown in blue in Fig. 6. Initially, on decreasing the extension, the blue trace falls on top of the naked DNA traces (green and black). However, for extensions less than about 1320 nm, the blue trace deviates from the naked DNA traces, indicative of nucleosome rewinding at sufficiently low forces. The blue curve and the red curve do not fall on top of each other at low forces because several of the 12 nucleosomes initially present dissociated at high force and were therefore unavailable to undergo rewinding when the force was subsequently decreased.

Previously unwound mononucleosomes show the canonical mononucleosome force *versus* extension curves after rewinding

Claudet *et al.* have suggested that unwound nucleosomes under tension may suffer partial octamer disassembly via H2A–H2B dimer dissociation.[58] An important difference between the procedures of Ref. 58 and the present work is that the maximum force applied in Ref. 58 (40 pN) was much higher than that in the present work (15 pN). Nevertheless, we sought to examine the behavior of previously unwound nucleosomes under our experimental conditions to check that they show the canonical nucleosome force *versus* extension behavior. We reasoned as in Ref. 19 that such behavior is compelling evidence of a properly formed nucleosome, that is, if a nucleosome that had previously unwound into state 0 subsequently displays the canonical nucleosome force *versus* extension behavior, it must have properly formed upon rewinding and did not lose H2A–H2B. Further support for the assertion that the low-force transition depends critically on a properly constituted nucleosome follows from the nucleosome structure, which reveals that the histone–DNA contacts involved in the nucleosome outer turn are H2A–H2B–DNA contacts.[23,59]

To carry out this test, we chose to examine single nucleosomes—mononucleosomes—for two reasons. First, the 2→1 transition is especially unambiguous for mononucleosomes.[18,19] Second, examining a mononucleosome represents a stringent test because of how we create

the mononucleosome. To create a mononucleosome, we carried out repeated force-extension measurements on the same tether. During this process, the number of nucleosomes progressively decreased because of dissociation, so that after several iterations, a mononucleosome remained, whose force *versus* extension could then be compared to the canonical mononucleosome force *versus* extensions of Refs. 18 and 19. Therefore, prior to measurements, the mononucleosome had previously been in state 0 several times. As exemplified in Fig. 7, each time such a previously unwound mononucleosome was pulled, it showed the canonical mononucleosome force *versus* extension curve,[18,19] in which the 2→1 transition occurs at low force and the 1→0 transition occurs at high force, entirely consistent with a properly formed nucleosome. The blue trace in Fig. 7 corresponds to relaxing the mononucleosome, starting in state 0 and then reducing the extension to zero. The trace that is shown in distinct tan, red, and purple segments corresponds to the mononucleosome's subsequent extension. The tan segment of the trace corresponds to a properly formed, fully wrapped nucleosome in nucleosome state 2; the red segment of the trace corresponds to state 1; and the purple segment of the traces corresponds to state 0. The 2→1 transition near 2 pN, separating tan and red portions of the trace, is unambiguous. These and additional analogous measurements clearly indicate the existence of a properly formed nucleosome at low force (state 2), even through the nucleosome in question had been unfolded previously into state 0 multiple times.

Force-clamp procedure to measure the unwinding and rewinding rates

To measure unwinding/rewinding rates at fixed force, we implemented a proportional–integral–derivative feedback controller using LabVIEW™, in which the force is held constant by adjusting the position of the piezoelectric stage—a force clamp. In this way, we were able to study the extension as a function of time at fixed applied force, as is shown in Fig. 2. At each unwinding event, the force transiently decreases before returning to its force-clamp value, within about 15 ms (data not shown). The response time is limited by the resonance frequency of the microscope stage. Consequently, we can accurately measure rates up to about $30\,s^{-1}$.

To characterize unwinding of the nucleosome inner turn, we applied a force clamp for several forces between 5 and 15 pN and maintained it for between 100 and 1000 s, depending on the force. The force was then rapidly increased to 15 pN and held there for 1 s, which ensured unwinding of all nucleosomes and, by counting the number that unwind, permitted us to determine the total number of nucleosomes bound during each extension *versus* time trace. Over all forces, we have measured 265 unwinding times of wild-type nucleosomes from 56 different DNA molecules and 336 unwinding times of sin mutant nucleosomes from 59 different DNA molecules.

To characterize rewinding, first, we applied a force of 15 pN for 1 s, unwinding all initially wound nucleosomes into state 0. Then, the force was rapidly reduced to a force-clamp value between 1.8 and 4.7 pN and held there for between 10 and 40 s, depending on the force. At this final force-clamp value, we measured the extension as a function of time and observed rewinding events. We have measured 136 rewinding times of wild-type nucleosomes from 31 DNA molecules and 183 rewinding times of sin mutant nucleosomes from 32 DNA molecules.

At the lower forces within range of rewinding forces, it is possible in principle for a nucleosome to transition first from state 0 to state 1 and then from state 1 to state 2. The key reason why we can measure $k_{0\to1}$ without the measurement being confused by $k_{1\to2}$ is that, at each force, $k_{0\to1}$ is more than 10× faster than $k_{1\to2}$. Therefore, it is approximately the case that the 0→1 transition is complete for all nucleosomes before the 1→2 transition occurs for any nucleosome. This conclusion holds for both nucleosomes containing H4 and nucleosomes containing H4-R45H. Figure 8 shows three examples of extension *versus* time rewinding traces obtained for nucleosomes containing H4-R45H and illustrates that the two timescales for the different transitions can be readily separated. These data extend from 0 to 10 s after reducing the force abruptly from 15 pN to the force-clamp value of 2.35 pN. At the start of each trace, the extension is about 1220 nm, which is the expected length for DNA with nucleosomes in state 0 at 2.35 pN. Within the first second of each trace, the extension decreases rapidly in a stepwise fashion corresponding to each bound nucleosome undergoing the 0→1 transition. In addition to these events at times within 1 s, Fig. 8b shows an additional step down near 4 s, while Fig. 8c shows first a step down near 7 s and a subsequent

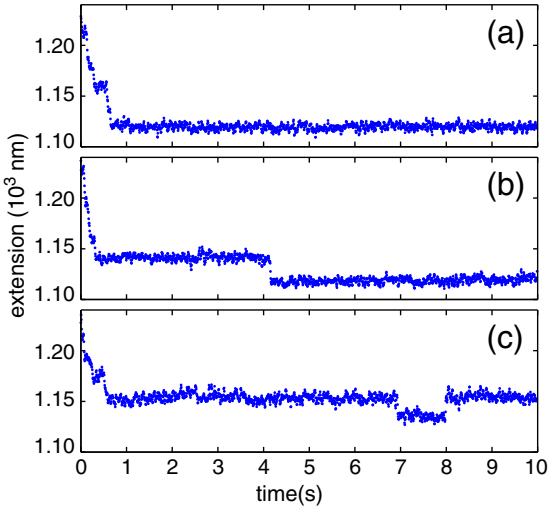

Fig. 8. Comparison of several extension *versus* time traces, measured at a fixed force of 2.35 pN, for nucleosomes containing H4-R45H. Between 0 and 1 s, each trace shows a number of steps down in extension, corresponding to the 0→1 transition. These early-time steps are the only feature of trace (a). In trace (b), however, there is an additional step down at 4 s, which we identify with the 1→2 transition of one of the nucleosomes at 2.35 pN. In trace (c), there is an additional step down at 7 s, which we identify with the 1→2 transition of one of the nucleosomes into the fully wound state (state 2), followed at about 8 s by a step up, corresponding to the 2→1 transition of the previously fully wound nucleosome.

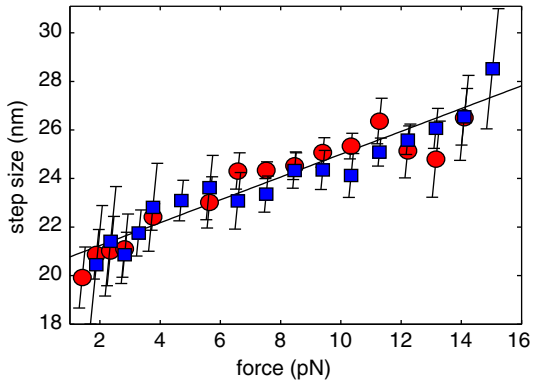

Fig. 9. Mean step size as a function of force, for nucleosomes containing H4 (squares) and nucleosomes containing H4-R45H (circles), determined from steps in extension in our force-clamp traces. The line is a least-mean-square fit of these data to a straight line. The error bars represent the standard deviation of the distribution of step sizes at each force.

step up near 8 s. Because these later transitions occur on much longer timescales than the 0→1 transitions, we identify the later steps down with the 1→2 transition and the step up with the 1→2 transition. From these and additional rewinding traces, we estimate that $k_{1\to2}=0.04\pm0.05\,s^{-1}$ at 2.35 pN. By contrast, $k_{0\to1}=2.0\pm0.3\,s^{-1}$, which is more than 40-fold faster.

To avoid as far as possible the inclusion of 1→2 transitions in our determination of $k_{0\to1}$, we restricted the time range considered to times between 0 and the shorter of $2/k_{0\to1}$ and 20 s. With this restriction, it is straightforward to show that we may expect less than 3% of the included steps to actually correspond to the 1→2 transition, leading to a negligible contribution to the error in our determination of $k_{0\to1}$.

Determination of unwinding times and step sizes

To determine the step times and sizes, we implemented a simple step-finding procedure that reliably determines the unwinding times for each data trace. Steps were detected by a force change greater than 0.1 pN coincident with a change in length of greater than 10 nm. The step size was determined by the difference of the mean extension from 40 ms before the step to the step and from the step to 40 ms after the step. In the case of fast unwinding, the 40-ms average is replaced by an average over the time to the nearest step. The black lines in Fig. 2 correspond to the so-obtained steps. The mean step size and its standard deviation are plotted *versus* force in Fig. 9, showing good agreement with the step sizes found for unwinding the nucleosome inner turn in previous reports.[14,15,18,19] We do not observe any steps near 50 nm.

Maximum-likelihood estimate of the unwinding rate

To determine the unwinding and rewinding rates for the nucleosome inner turn at fixed force from the collection of measured transition times, we employ a maximum-likelihood method that is a modified version of the approach described in Ref. 60. We consider a strand of DNA with N initially wound nucleosomes. Force is rapidly applied until the force reaches a fixed value. During the initial force increase, each nucleosome outer turn unwinds so that, at time $t=0$, when the force first achieves the force-clamp value, each nucleosome is in state 1 (Fig. 7a). The force is then held constant for a total time t. Between $t=0$ and time t, the inner turn around n of the nucleosomes unwinds ($n\le N$). Assuming that each nucleosome unwinds independently and that the nucleosome unwinding rate is k, the probability that n nucleosomes unwind in a total time t, the first within dt_1 of time t_1, the second within dt_2 of time t_2, and so on, and nucleosome n unwinds within dt_n of t_n is equal to

$$P=N(N-1)\ldots(N-n+1)k^n e^{-k(t_1+t_2+\ldots t_n+(N-n)t)}dt_1dt_2\ldots dt_n \tag{10}$$

where dt_1, dt_2, and so on are infinitesimal ranges of time. In our experiments, the unwinding times and the value of N for each trace are measured.

Given a trace of total duration t, containing a set of experimental unwinding times, $t_1,t_2,\ldots t_n$, we determine the unwinding rate k as the value that maximizes P. The maximum of P and the maximum of $\ln P$ occur at the same value of k, making it convenient to determine the maximum-likelihood value of k by maximizing $\ln P$ with respect to k, that is, we set

$$\frac{d\ln P}{dk}=0 \tag{11}$$

Substituting Eq. (10) into Eq. (11), we find

$$\frac{n}{\bar{k}}-t_1-t_2\ldots-t_n-(N-n)t=0 \tag{12}$$

Thus,

$$\bar{k}=\frac{n}{t_1+t_2\ldots+t_n+(N-n)t} \tag{13}$$

where $\bar{k}$ is the maximum-likelihood value of the nucleosome unwinding rate for a single experimental trace.

For a collection of separate traces, the appropriate probability is simply the product of the probabilities for each trace in the collection. Thus, for a collection of m traces, we have

$$P=P^{(1)}P^{(2)}\ldots P^{(m)} \tag{14}$$

and Eq. (11) becomes

$$\frac{d\ln P^{(1)}}{dk}+\frac{d\ln P^{(2)}}{dk}\ldots+\frac{d\ln P^{(m)}}{dk}=0 \tag{15}$$

It follows, in this case, that the maximum-likelihood value of k ($\bar{k}$) is given by

$$\bar{k}=\frac{n^{(1)}\ldots.+n^{(m)}}{t_1^{(1)}+t_2{}^{(1)}\ldots.+t_{n^{(1)}}^{(1)}+(N^{(1)}-n^{(1)})t^{(1)}\ldots..+t_1^{(m)}+t_2^{(m)}\ldots.+t_{n^{(m)}}^{(m)}+(N^{(m)}-n^{(m)})t^{(m)}} \tag{16}$$

where $n^{(q)}$ is the number of unwinding events for trace q, $t_p^{(q)}$ is unwinding time p of trace q, $N^{(q)}$ is the initial number

of bound nucleosomes for trace q, and $t^{(q)}$ is the total duration of trace q. To calculate the maximum-likelihood values of $k_{1\to0}$ and $k_{0\to1}$ from our experimental data, we use Eq. (16).

However, if all nucleosomes unwind within the observation time so that $n^{(q)}=N^{(q)}$ for every experimental trace, it is interesting to note that we may drop the index q, and Eq. (16) simplifies

$$\bar{k} = \frac{N}{t_1 + t_2 + \ldots + t_i + \ldots + t_N} \tag{17}$$

In Eq. (17), t_i is the time at which nucleosome i unwinds, irrespective of the particular trace in which it occurs, and N is the total number of nucleosome unwinding events in all experimental traces at a given force.

For an exponential distribution of step times, we may expect the distribution of the mean of the step times to follow a gamma distribution. On this basis, the expected standard deviation in the mean step time is equal to the mean divided by the square root of the number of steps. It then follows from Eq. (17) that the expected standard deviation of $\bar{k}$ is equal to $\sigma_{\bar{k}} = \bar{k} / \sqrt{N}$.

Fluctuations in the number of unwound nucleosomes

In this section, we examine whether the deviations between our measurements and single-exponential behavior are consistent with the statistical errors that may be expected under our experimental conditions.

For a population of N initially wound nucleosomes under force, the probability that a particular nucleosome is unwound at time t is

$$p = 1-e^{-kt} \tag{18}$$

where k is the nucleosome unwinding rate for the force in question. Because at any time a given nucleosome is either wound or unwound, the probability (Q) that m nucleosomes out of the total population of N nucleosomes are unwound at time t is given by the binomial distribution:

$$Q = \frac{N!}{m!(N-m)!} p^m (1-p)^{N-m} \tag{19}$$

It follows from the properties of the binomial distribution that mean fraction of unwound nucleosomes at time t is

$$\frac{<m>}{N} = \frac{Np}{N} = 1-e^{-kt} \tag{20}$$

and that the fractional standard deviation in the number of unwound nucleosomes at time t is

$$\frac{\sigma_m}{N} = \sqrt{\frac{Np(1-p)}{N}} = \sqrt{\frac{e^{-kt}(1-e^{-kt})}{N}} \tag{21}$$

The hatched regions in Fig. 10 is bounded by curves given by $(<m>\pm2\sigma_m)/N$. We may expect traces to lie within these bounds 95% of the time, which is certainly the case for the traces shown.

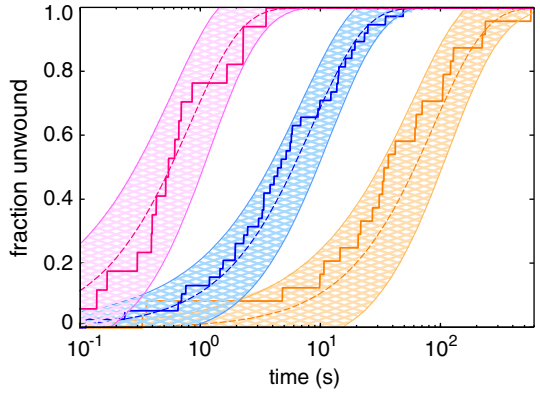

Fig. 10. Fraction of nucleosomes unwound *versus* time, showing experimental data (stepwise continuous lines), and the expected mean fraction unwound for the maximum-likelihood unwinding rate (broken curve). The 2-SD range of the fraction unwound is shown as the hatched region. These data correspond to nucleosomes containing H4-R45H at 9.4 pN (magenta), 8.5 pN (blue), and 6.6 pN (orange).

Acknowledgement

We thank the members of the Regan and Mochrie laboratories and M. Hochstrasser for valuable discussions. We thank C. Cheng and R. Salinas for their contributions to this research. This work was supported by the Raymond and Beverly Sackler Institute for Biological, Physical and Engineering Sciences and the National Science Foundation Physics of Living Systems grant 1019147. D.J.S. is the recipient of a National Science Foundation Graduate Research Fellowship.

Author contributions. D.J.S. and A.H.M. contributed equally to this work. D.J.S. and A.H.M. performed experiments and conducted data analyses. D.J.S. and R.P.I. purified proteins, and D.J.S. prepared DNA. A.H.M. and S.G.J.M. designed and built the optical tweezer apparatus. A.H.M., D.J.S., R.P.I., L.R., and S.G.J.M. conceived experiments and analyses and cowrote the manuscript.

References

1. Williams, S. K. & Tyler, J. K. (2007). Transcriptional regulation by chromatin disassembly and reassembly. *Curr. Opin. Genet. Dev.* **17**, 88–93.
2. Saha, A., Wittmeyer, J. & Cairns, B. R. (2006). Chromatin remodelling: the industrial revolution of DNA around histones. *Nat. Rev., Mol. Cell Biol.* **7**, 437–447.
3. Segal, E., Fondufe-Mittendorf, Y., Chen, L., Thrastrom, A., Field, Y., Moore, I. K. *et al.* (2006). A genomic code for nucleosome positioning. *Nature*, **442**, 772–778.
4. Mitra, D., Parnell, E. J., Landon, J. W., Yu, Y. & Stillman, D. J. (2006). SWI/SNF binding to the HO

promoter requires histone acetylation and stimulates TATA-binding protein recruitment. *Mol. Cell. Biol.* **26**, 4095–4110.
5. Takahata, S., Yu, Y. & Stillman, D. J. (2011). Repressive chromatin affects factor binding at yeast HO (homothallic switching) promoter. *J. Biol. Chem.* **286**, 34809–34819.
6. Sternberg, P. W., Stern, M. J., Clark, I. & Hershkowitz, I. (1987). Activation of the yeast *HO* gene by release from multiple negative controls. *Cell*, **48**, 567–577.
7. Kruger, W., Peterson, C. L., Sil, A., Coburn, C., Arents, G., Moudrianakis, E. N. & Hershkowitz, I. (1995). Amino acid substitutions in the structured domains of histones H3 and H4 partially relieve the requirement of the yeast SWI/SNF complex for transcription. *Genes Dev.* **9**, 2770–2779.
8. Wechser, M. A., Kladde, M. P., Alfieri, J. A. & Peterson, C. L. (1997). Effects of Sin$^-$ versions of histone H4 on yeast chromatin structure and function. *EMBO J.* **16**, 2086–2095.
9. Muthurajan, U. M., Bao, Y., Forsberg, L. J., Edayathumangalam, R. S., Dyer, P. N., White, C. L. & Luger, K. (2004). Crystal structures of histone Sin mutant nucleosomes reveal altered protein–DNA interactions. *EMBO J.* **23**, 260–271.
10. Flaus, A., Rencurel, C., Ferreira, H., Wiechens, N. & Owen-Hughes, T. (2004). Sin mutations alter inherent nucleosome mobility. *EMBO J.* **23**, 343–353.
11. Kurumizaka, H. & Wolffe, A. P. (1997). Sin mutations of histone H3: influence on nucleosome core structure and function. *Mol. Cell. Biol.* **17**, 6953–6969.
12. Cui, Y. & Bustamante, C. (2000). Pulling a single chromatin fiber reveals the forces that maintain its higher-order structure. *Proc. Natl Acad. Sci. USA*, **97**, 127–132.
13. Bennink, M. L., Leuba, S. H., Leno, G. H., Zlatanova, J., de Grooth, B. G. & Greve, J. (2001). Unfolding individual nucleosomes by stretching single chromatin fibers with optical tweezers. *Nat. Struct. Biol.* **8**, 606–610.
14. Brower-Toland, B., Smith, C. L., Yeh, R. C., Lis, J. T., Peterson, C. L. & Wang, M. D. (2002). Mechanical disruption of individual nucleosomes reveals a reversible multistage release of DNA. *Proc. Natl Acad. Sci. USA*, **99**, 1960–1965.
15. Brower-Toland, B., Wacker, D. A., Fulbright, R. M., Lis, J. T., Kraus, W. L. & Wang, M. D. (2005). Specific contributions of histone tails and their acetylation to the mechanical stability of nucleosomes. *J. Mol. Biol.* **346**, 135–146.
16. Gemmen, G. J., Sim, R., Haushalter, K. A., Ha, P. C., Kadonaga, J. T. & Smith, D. E. (2005). Forced unravelling of nucleosomes assembled on heterogeneous DNA using core histones, NAP-1, and ACF. *J. Mol. Biol.* **351**, 89–99.
17. Pope, L. H., Bennink, M. L., van Leijenhorst-Groener, K. A., Nikova, D., Greve, J. & Marko, J. F. (2005). Single chromatin fiber stretching reveals physically distinct populations of disassembly events. *Biophys. J.* **88**, 3572.
18. Mihardja, S., Spakowitz, A. J., Zhang, Y. & Bustamante, C. (2006). Effect of force on mononucleosomal dynamics. *Proc. Natl Acad. Sci. USA*, **103**, 15871.
19. Kruithof, M. & van Noort, J. (2009). Hidden Markov analysis of nucleosome unwrapping under force. *Biophys. J.* **96**, 3708–3715.
20. Kruithof, M., Chien, F.-T., Routh, A., Logie, C., Rhodes, D. & van Noort, J. (2009). Single-molecule force spectroscopy reveals a highly compliant helical folding for the 30 nm chromatin fiber. *Nat. Struct. Mol. Biol.* **16**, 534.
21. Hall, M. A., Shundrovsky, A., Bai, L., Fulbright, R. M., Lis, J. T. & Wang, M. D. (2009). High-resolution dynamic mapping of histone–DNA interactions in a nucleosome. *Nat. Struct. Mol. Biol.* **16**, 124–129.
22. Simon, M., North, J. A., Shimko, J. C., Forties, R. A., Ferdinand, M. B., Manohar, M. *et al.* (2011). Histone fold modifications control nucleosome unwrapping and disassembly. *Proc. Natl Acad. Sci. USA*, **108**, 12711–12716.
23. Luger, K., Mader, A. W., Richmond, R. K., Sargent, D. F. & Richmond, T. J. (1997). Crystal structure of the nucleosome core particle at 2.8 Å resolution. *Nature*, **389**, 251–260.
24. Yodh, J., Lyubchenko, Y., Shlyakhtenko, L., Woodbury, N. & Lohr, D. (1999). Evidence for nonrandom behavior in 208–12 subsaturated nucleosomal array populations analyzed by AFM. *Biochemistry*, **38**, 15756–15763.
25. Miyagi, A., Ando, T. & Lyubchenko, Y. (2011). Dynamics of nucleosomes assessed with time-lapse high speed atomic force microscopy. *Biochemistry*, **50**, 7901–7908.
26. Kulic, I. M. & Schiessel, H. (2004). DNA spools under tension. *Phys. Rev. Lett.* **92**, 228101.
27. Thastrom, A., Gottesfeld, J. M., Luger, K. & Widom, J. (2004). Histone–DNA binding free energy cannot be measured in dilution-driven dissociation experiments. *Biochemistry*, **43**, 736–741.
28. Zhang, Y., Smith, C. L., Saha, A., Grill, S. W., Mihardja, S., Smith, S. B. *et al.* (2006). DNA translocation and loop formation mechanism of chromatin remodeling by SWI/SNF and RSC. *Mol. Cell*, **24**, 559–568.
29. Li, B., Carey, M. & Workman, J. L. (2007). The role of chromatin during transcription. *Cell*, **128**, 707–719.
30. Sudhanshu, B., Mihardja, S., Koslover, E. F., Mehraeen, S., Bustamante, C. & Spakowitz, A. J. (2011). Tension-dependent structural deformation alters single-molecule transition kinetics. *Proc. Natl Acad. Sci. USA*, **108**, 1885–1890.
31. Tinoco, I. & Bustamante, C. (2002). The effect of force on thermodynamics and kinetics of single molecule reactions. *Biophys. Chem.* **102**, 513–533.
32. Kulić, I. M., Mohrbach, H., Thaokar, R. & Schiessel, H. (2007). Equation of state of looped DNA. *Phys. Rev. E: Stat. Phys., Plasmas, Fluids, Relat. Interdiscip. Top.* **75**, 011913.
33. Jenuwein, T. & Allis, C. D. (2001). Translating the histone code. *Science*, **293**, 1074–1080.
34. Fraga, M. F. & Esteller, M. (2005). Towards the human cancer epigenome: a first draft of histone modifications. *Cell Cycle*, **4**, 1377–1381.
35. Allfrey, V. G., Faulkner, R. & Mirsky, A. E. (1964). Acetylation and methylation of histones and their possible role in the regulation of RNA synthesis. *Proc. Natl Acad. Sci. USA*, **51**, 786–794.
36. Pogo, B. G., Pogo, A. O., Allfrey, V. G. & Mirsky, A. E. (1968). Changing patterns of histone acetylation and RNA synthesis in regeneration of the liver. *Proc. Natl Acad. Sci. USA*, **59**, 1337–1344.

37. Wang, G. G., Allis, C. D. & Chi, P. (2007). Chromatin remodeling and cancer. Part I: covalent histone modifications. *Trends Mol. Med.* **13**, 363–372.
38. Ausió, J. (2006). Histone variants—the structure behind the function. *Brief. Funct. Genomic. Proteomic.* **5**, 228–243.
39. Montel, F., Menoni, H., Castelnovo, M., Bednar, J., Dimitrov, S., Angelov, D. & Faivre-Moskalenko, C. (2009). The dynamics of individual nucleosomes controls the chromatin condensation pathway: direct atomic force microscopy visualization of variant chromatin. *Biophys. J.* **97**, 544–553.
40. Henikoff, S. (2008). Nucleosome destabilization in the epigenetic regulation of gene expression. *Nat. Rev., Genet.* **9**, 15–26.
41. Iizuka, M. & Smith, M. M. (2003). Functional consequences of histone modifications. *Curr. Opin. Genet. Dev.* **13**, 154–160.
42. Lowary, P. T. & Widom, J. (1998). New DNA sequence rules for high affinity binding to histone octamer and sequence-directed nucleosome positioning. *J. Mol. Biol.* **276**, 19–42.
43. Thastrom, A., Lowary, P. T., Widlund, H. R., Cao, H., Kubista, M. & Widom, J. (1999). Sequence motifs and free energies of selected natural and non-natural nucleosome positioning DNA sequences. *J. Mol. Biol.* **288**, 213–229.
44. Takahata, S., Yu, Y. & Stillman, D. J. (2009). FACT and Asf1 regulate nucleosome dynamics and coactivator binding at the HO promoter. *Mol. Cell*, **34**, 405–415.
45. Jackrel, M. E., Valverde, R. & Regan, L. (2009). Redesign of a protein–peptide interaction: characterization and applications. *Protein Sci.* **18**, 762–774.
46. Cortajarena, A. L., Yi, F. & Regan, L. (2008). Designed TPR modules as novel anticancer agents. *ACS Chem. Biol.* **3**, 161–166.
47. Cortajarena, A. L., Kajander, T., Pan, W., Cocco, M. J. & Regan, L. (2004). Protein design to understand peptide ligand recognition by tetratricopeptide repeat proteins. *Protein Eng. Des. Sel.* **17**, 399–409.
48. Luger, K., Rechsteiner, T. J. & Richmond, T. J. (1999). Expression and purification of recombinant histones and nucleosome reconstitution. *Methods Mol. Biol.* **119**, 1–16.
49. Holmberg, A., Blomstergren, A., Nord, O., Lukacs, M., Lundeberg, J. & Uhlen, M. (2005). The biotin–streptavidin interaction can be reversibly broken using water at elevated temperatures. *Electrophoresis*, **26**, 501–510.
50. Fuller, D. N., Gemmen, G. J., Rickgauer, J. P., Dupont, A., Millin, R., Recouvreux, P. & Smith, D. E. (2006). A general method for manipulating DNA sequences from any organism with optical tweezers. *Nucleic Acids Res.* **34**, e15.
51. Schlingman, D. J., Mack, A. H., Mochrie, S. G. J. & Regan, L. (2011). A new method for the covalent attachment of DNA to a surface for single-molecule studies. *Colloids Surf., B*, **83**, 91–95.
52. Finzi, L. & Gelles, J. (1995). Measurement of lactose repressor-mediated loop formation and breakdown in single DNA molecules. *Science*, **267**, 5196.
53. Huynh, V. A., Robinson, P. J. & Rhodes, D. (2005). A method for the *in vitro* reconstitution of a defined 30 nm chromatin fibre containing stoichiometric amounts of the linker histone. *J. Mol. Biol.* **345**, 957–968.
54. Gittes, F. & Schmidt, C. F. (1998). interference model for back-focal-plane displacement detection in optical tweezers. *Opt. Lett.* **23**, 7–9.
55. Berg-Sørensen, K. & Flyvbjerg, H. (2004). Power spectrum analysis for optical tweezers. *Rev. Sci. Instrum.* **75**, 594–612.
56. Deufel, C. & Wang, M. D. (2006). Detection of forces and displacements along the axial direction in an optical trap. *Biophys. J.* **90**, 657–667.
57. Chen, Y.-F., Blab, G. A. & Meiners, J.-C. (2009). Stretching submicron biomolecules with constant-force axial optical tweezers. *Biophys. J.* **96**, 4701–4708.
58. Claudet, C., Angelov, D., Bouvet, P., Dimitroov, S. & Bednar, J. (2005). Histone octamer instability under single molecule experiment conditions. *J. Biol. Chem.* **280**, 19958–19965.
59. Davey, C. A., Sargent, D. F., Luger, K., Maeder, A. W. & Richmond, T. J. (2002). Solvent mediated interactions in the structure of the nucleosome core particle at 1.9 Å resolution. *J. Mol. Biol.* **319**, 1097–1113.
60. Brujic, J., Hermans, R. I., Walther, K. A. & Fernandez, J. M. (2006). Single-molecule force spectroscopy reveals signatures of glassy dynamics in the energy landscape of ubiquitin. *Nat. Phys.* **2**, 282–285.